

Table 1: HSI completion results (RSE) under three different tensor orders with different rank selections

	TRLRF	TRALS	TRWOPT	TMac	TenALS	t-SVD	FBCP	HaLRTC
3-order, high-rank( $R_n = 12$ )	<b>0.06548</b>	0.07049	0.06695	0.1662	0.3448	0.4223	0.2363	0.1254
3-order, low-rank( $R_n = 8$ )	<b>0.1166</b>	0.1245	0.1249	0.2963	0.3312	-	-	-
5-order, high-rank( $R_n = 22$ )	<b>0.1035</b>	0.1392	0.1200	0.8064	-	0.9504	0.3833	0.3944
5-order, low-rank( $R_n = 18$ )	<b>0.1062</b>	0.1122	0.1072	0.7411	-	-	-	-
8-order, high-rank( $R_n = 24$ )	<b>0.1190</b>	0.1319	0.1637	0.9487	-	0.9443	0.4021	0.9099
8-order, low-rank( $R_n = 20$ )	<b>0.1421</b>	0.1581	0.1767	0.9488	-	0.9450	0.4135	0.9097

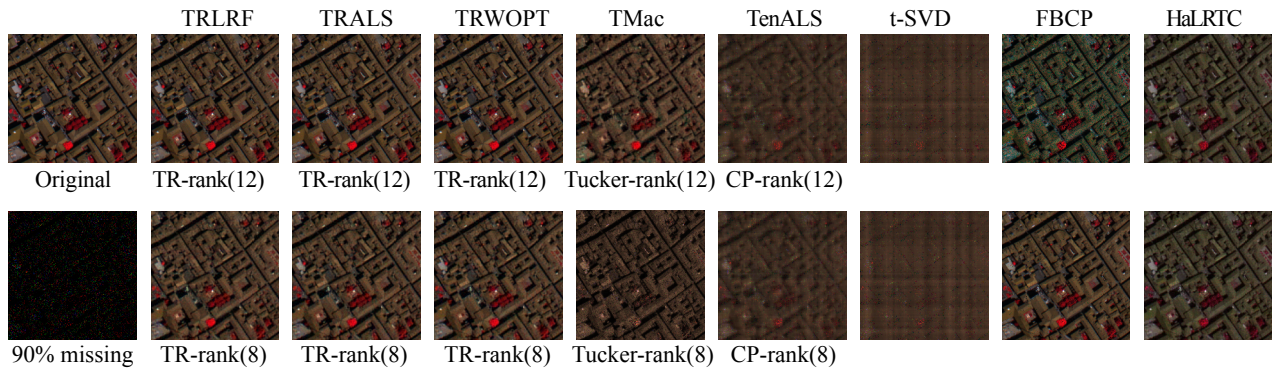


Figure 6: Completion results under the 0.9 missing rate HSI data. The channels 80, 34, 9 are picked to show the visual results. The rank selection of TRLRF, TRALS, TRWOPT, TMac and TenALS are given under the corresponding images.

## Hyperspectral image

A hyperspectral image (HSI) of size  $200 \times 200 \times 80$  which records an area of the urban landscape was tested in this section<sup>1</sup>. In order to test the performance of TRLRF on higher-order tensors, the HSI data was reshaped to higher-order tensors, which is an easy way to find more low-rank features of the data. We compared our TRLRF to the other seven tensor completion algorithms in 3-order tensor ( $200 \times 200 \times 80$ ), 5-order tensor ( $10 \times 20 \times 10 \times 20 \times 80$ ) and 8-order tensor ( $8 \times 5 \times 5 \times 8 \times 5 \times 5 \times 8 \times 10$ ) cases. The higher-order tensors were generated from original HSI data by directly reshaping it to the specified size and order.

The experiment aims to verify the completion performance of the eight algorithms under different model selection, whereby the experiment variables are the tensor order and tensor rank. The missing rates of all the cases are set as 0.9. All the tuning parameters of every algorithm were set according to the statement in the previous experiments. Besides, for the experiments which need to set rank manually, we chose two different tensor ranks: high-rank and low-rank for algorithms. It should be noted that the CP-rank of TenALS and the Tucker-rank of TMac were set to the same values as TR-rank. The completion performance of RSE and visual results are listed in Table 1 and shown in Figure 6. The results of FBCP, HaLRTC and t-SVD were not affected by tensor rank, so the cases of the same order with different rank are left blank in Table 1. The TenALS could not deal with tensor more than three-order, so the high-order

tensor cases for TenALS are also left blank. As shown in Table 1, our TRLRF gives the best recovery performance for the HSI image. In the 3-order cases, the best performance was obtained when the TR-rank was 12, however, when the rank was set to 8, the performance of TRLRF, TRALS, TRWOPT, TMac, and TenALS failed because of the underfitting of the selected models. For 5-order cases, when the rank increased from 18 to 22, the performance of TRLRF kept steady while the performance of TRALS, TRWOPT, and TMac decreased. This is because the high-rank makes the models overfit while our TRLRF performs without any issues, owing to its inherent TR-rank robustness. In the 8-order tensor cases, similar properties can be obtained and our TRLRF also performed the best.

## Conclusion

We have proposed an efficient and high-performance tensor completion algorithm based on TR decomposition, which employed low-rank constraints on the TR latent space. The model has been efficiently solved by the ADMM algorithm and it has been shown to effectively deal with model selection which is a common problem in most traditional tensor completion methods, thus providing much lower computational cost. The extensive experiments on both synthetic and real-world data have demonstrated that our algorithm outperforms the state-of-the-art algorithms. Furthermore, the proposed method is general enough to be extended to various other tensor decompositions in order to develop more efficient and robust algorithms.

<sup>1</sup>[http://www.ehu.eus/ccwintco/index.php/Hyperspectral\\_Remote\\_Sensing\\_Scenes](http://www.ehu.eus/ccwintco/index.php/Hyperspectral_Remote_Sensing_Scenes)